Multiple areas of acute vision in two freshwater teleosts, the creek chub, *Semotilus atromaculatus* (Mitchill) and the cutlips minnow, *Exoglossum maxillingua* (Lesueur)

SHAUN P. COLLIN[1]
Department of Psychology, University of Western Australia, Nedlands 6009, Western Australia, Australia
and
Département de Biologie, Université de Montréal, C.P. 6128, Succursale A, Montréal, PQ H3C 3J7, Canada
AND
M. ATHER ALI
Département de Biologie, Université de Montréal, Succursale A, Montréal, PQ H3C 3J7, Canada

Received July 30, 1993
Accepted February 4, 1994

COLLIN, S.P., and ALI, M.A. 1994. Multiple areas of acute vision in two freshwater teleosts, the creek chub, *Semotilus atromaculatus* (Mitchill) and the cutlips minnow, *Exoglossum maxillingua* (Lesueur). Can. J. Zool. **72**: 721–730.

The topography of Nissl-stained cells within the retinal ganglion cell layer is examined in two closely related freshwater teleosts from the family Cyprinidae. Regardless of the close phylogenetic relationship and the sympatric habitats of the two species, pronounced differences in the number and position of areas of increased cell density are observed in their retinae. in the creek chub, *Semotilus atromaculatus*, a midwater crepuscular feeder, three retinal specializations or areae centrales are identified in the dorsonasal, nasal, and temporal regions of the retina. In the cutlips minnow, *Exoglossum maxillingua*, a benthic diurnal feeder, two areae centrales are identified in temporal and nasal retina. The upper limits of the spatial resolving power of each species are calculated from the spacing of cells within the ganglion cell layer. Differences in the arrangement of isodensity contours appear to reflect the symmetry of each species' visual environment. The development and significance of up to three visually acute zones are discussed.

COLLIN, S.P., et ALI, M.A. 1994. Multiple areas of acute vision in two freshwater teleosts, the creek chub, *Semotilus atromaculatus* (Mitchill) and the cutlips minnow, *Exoglossum maxillingua* (Lesueur). Can. J. Zool. **72** : 721–730.

La topographie des cellules sensibles au Nissl dans la couche de cellules ganglionnaires de la rétine a fait l'objet d'une étude chez deux espèces très apparentées de téléostéens de la famille des Cyprinidae. En dépit de leur lien de parenté phylogénétique étroit et de leur choix d'habitats sympatriques, il existe entre les deux espèces des différences importantes quant au nombre et à la position des zones rétiniennes à densité cellulaire plus grande. Chez le Mulet à cornes, *Semotilus atromaculatus*, qui s'alimente au milieu de la colonne d'eau au crépuscule, trois zones centrales de spécialisations rétiniennes peuvent être reconnues dans les régions dorso-nasale, nasale et temporale de la rétine. Chez le Bec-de-lièvre, *Exoglossum maxillingua*, qui s'alimente dans la zone benthique le jour, seulement deux zones centrales de spécialisation prévalent, l'une dans la rétine nasale, l'autre dans la rétine temporale. La limite supérieure du pouvoir de résolution spatiale a été calculée chez chacune des espèces par évaluation de l'espacement entre les cellules de la couche ganglionnaire. Des différences dans l'arrangement des profils d'isodensité semblent refléter la symétrie de l'environnement visuel de chacune des espèces. L'importance évolutive et la raison d'être de trois zones d'acuité visuelle particulière font l'objet d'une discussion.
[Traduit par la Rédaction]

Introduction

The topographic distribution of retinal ganglion cells has been extensively studied in a number of non-teleost vertebrate phyla, including man (Hughes 1975, 1977; Vaney 1980; Dunlop and Beazley 1981; Hebel and Hollander 1983; Wong et al. 1986). The earliest studies in teleosts (Slonaker 1897; Kahmann 1934, 1935; Munk 1970) compared different classes of fish possessing obvious retinal specializations such as foveae and ridges across the horizontal meridian of the eye. However, all of these were qualitative studies. More recently, a range of marine teleosts has been subjected to quantitative analyses, revealing a rich diversity in both the density of retinal elements, the arrangement of the isodensity contours, and the relative positions of areas of acute vision, defined as regions of increased photoreceptor and (or) ganglion cell density (Yamanouchi 1956; O'Connell 1963; Schwassmann 1968; Ahlbert 1976; Ito and Murakami 1984; Collin and Pettigrew 1988*a*, 1988*b*, 1988*c*; Collin and Collin 1988; Kawamura and Ohashi 1988; Collin 1989).

Freshwater teleosts have received relatively little attention (Fernald and Johns 1980; Zaunreiter et al. 1991), with the notable exception of the goldfish *Carassius auratus* (Cyprinidae). Early studies showed that the retina of *C. auratus* possesses a homogeneous population of retinal ganglion cells (Johns and Easter 1977; Kock and Reuter 1978; Murray et al. 1982), but more recently a slight increase in the density of both ganglion (Mednick and Springer 1988) and photoreceptor (Mednick et al. 1988) cells in the temporal retina has been described. Given that other, less inbred cyprinid species possess multiple areas of increased photoreceptor density (Zaunreiter et al. 1991), we decided to investigate the topography of cells within the ganglion cell layer of two wild cyprinid species.

The two sympatric species, *Semotilus atromaculatus* (Cyprinidae) and *Exoglossum maxillingua* (Cyprinidae), were chosen for analysis because of their different habitats, feeding strategies, and peak periods of feeding activity. Species were collected in their natural habitat, a landlocked Laurentian

[1]Author to whom correspondence should be sent at the following address: Department of Zoology, University of Western Australia, Nedlands 6009, Western Australia, Australia.

Printed in Canada / Imprimé au Canada

Shield lake, to investigate interspecific variations of retinal topography without the inherent problems of interbreeding and also to test the hypothesis that differences in retinal ultrastructure (Collin et al.[2,3]) and the morphological relationship of the two eyes to the mouth (Scott and Crossman 1973) are reflected in the arrangement of retinal ganglion cells, even though, to some extent, the two species utilize the same food source (Barber and Minckley 1971; Pappantoniou et al. 1984*a*).

The creek chub, *S. atromaculatus*, is arguably one of the most common stream minnows in North America. It is a visual feeder that prefers the clear warm and turbid waters of streams and brooks but may also frequent the shore waters of small lakes. This species occupies the mid to upper layers of the water column and relies on increasing its predatory activity at night rather than risk early detection by its prey or by potential predators under brighter conditions (Cerri 1983). *Semotilus atromaculatus* is omnivorous, consuming planktonic organisms when young and eating insect larvae, beetles, mayflies, and caddisflies as adults. The changes in its diet during growth culminate in heavy predation of the juveniles of other fish species as an adult (Barber and Minckley 1971). Large adult males have also been reported to eat crayfish and small fishes (Scott and Crossman 1973), while cladocerans, algae, and higher plant tissues also constitute a significant part of the diet (Dinsmore 1962). They feed efficiently in schools or individually at all levels, although predominantly in the mid to upper levels of the water column. Feeding occurs primarily during periods of low light intensity (Cerri 1983), although younger individuals are found to consume prey throughout the day in the northern regions of the United States (Copes 1978). *Semotilus atromaculatus* is considered to be a sight feeder (Evans 1952), having poorly developed cutaneous sense organs and only a rudimentary pair of maxillary barbels. The sight-feeding hypothesis is confirmed upon examination of the brain of this species, which reveals a reduction in the size of the facial and vagal lobes but a large optic tectum (Evans 1952). Owing to the preferred position of this species in the upper layers of the water column, it is consumed by a variety of natural predators such as loons, kingfishers, and mergansers (Scott and Crossman 1973).

A large amount of work has concentrated on the morphology (Scott and Crossman 1973) and life history (Magnan and FitzGerald 1984*a*) of *S. atromaculatus*, including studies on nest building (Reighard 1910), reproductive behaviour (Dobie et al. 1956; Copes 1978), growth (Dinsmore 1962), and feeding (Barber and Minckley 1971). Investigations of the visual behaviour of this species have been restricted to the effects of light intensity on feeding (Magnan and FitzGerald 1982, 1984*a*, 1984*b*; Cerri 1983) and examination of the scotopic visual pigments (Heinermann and Ali 1989) and of the photoacoustic spectra of the visual pigment porphyropsin at low temperatures (Yoon et al. 1988).

The cutlips minnow, *E. maxillingua*, is also common, although it is more confined to the northeastern regions of the United States and Canada. It is a benthic diurnal forager of insect larvae and molluscs (Johnson 1981, 1982) and is found on gravelly bottoms in clear, slow-moving streams and lakes that are relatively free of rooted plants and silt. Smaller fish prefer chironomid larvae, while larger fish prey upon trichopteran larvae (Johnson 1982). Unlike the creek chub, this species is a sluggish bottom dweller and can often be found hidden under stones in quiet pools. The mouth of the cutlips minnow is adapted for feeding off the bottom, the lower jaw consisting of three lobes, the centre one being raised and tonguelike (Scott and Crossman 1973). This modification of the mouthparts has also been reported to facilitate eye-picking behaviour, especially against prey with large or uncamouflaged eyes (Johnson 1981). *Exoglossum maxillingua* is a diurnal species with activity peaks occurring after dawn and near dusk.

Other studies of *E. maxillingua* have concentrated on diet (Johnson 1981), breeding (Hankinson 1922; Van Duzer 1939), life history (Pappantoniou et al. 1984*a*, 1984*b*), and development (Fuiman and Loos 1978). The only reference to visual behaviour in this species is that of Heinermann and Ali (1985), who found that the spectral sensitivity of porphyropsin matches the spectral composition of the surrounding water.

The aim of this study was to compare the topography of cells within the ganglion cell layer of *S. atromaculatus* (a noctural feeder) and *E. maxillingua* (a diurnal scotopic feeder). The two species are members of the same family and live sympatrically within the same ecosystem but occupy different ecological niches, allowing interspecific variation to be examined.

Methods

Ten adult creek chubs, *Semotilus atromaculatus* (Mitchill) 92–117 mm total length) and 10 adult cutlips minnows, *Exoglossum maxillingua* (Lesueur) (90–110 mm total length) were collected from Lake Cromwell, at the biological station of the Université de Montréal, near St. Hyppolyte, Quebec, Canada. Collections were made between December 1988 and February 1989, when the lake was covered by approximately 1 m of ice. To immerse the fish traps, a number of holes (0.5 m in diameter) were bored using a diesel-powered auger and a steel crowbar. Five fish traps, each consisting of a plastic basket (0.25 m long and 0.15 m wide) with a funnel-shaped opening at each end, were filled with bread and lowered to either lie on the bottom (1–3 m) or be suspended midwater (2 m) and then left overnight. The following day, accumulated ice was removed and the traps were retrieved. Each specimen was then transferred to an aerated tank which was transported via snowmobile to the laboratories of the biology station.

For all specimens, sampling was carried out according to the ethical guidelines of the National Health and Medical Research Council of Australia. Two individuals of each species were immersed in an overdose of tricaine methane sulphonate (MS 222, 1:2000) and the eyes excised. Following the removal of the cornea, lens, and vitreous, the eyecup was immersed in 4% paraformaldehyde in phosphate buffer (0.1 M) overnight. Small retinal pieces cut from various regions of the fundus were then washed in phosphate buffer and embedded in Historesin (Reichert-Jung). Sections (1–2 μm) were cut using an American Optical microtome and a steel knife. Sections were stained with either toluidine blue or Richardson's stain and dehydrated, and a cover slip was applied, for analysis with a compound light microscope (Olympus, BH-2).

The remaining eight individuals of each species were used for the preparation of retinal whole-mounts. After 3 h of dark adaptation, each eye was excised under MS 222 anaesthesia (1:2000), its cornea, lens, and vitreous were removed under a red safe light, and the eyecup

[2]S.P. Collin, H.B. Collin, and M.A. Ali. 1994. Fine structure of the duplex retina in the creek chub, *Semotilus atromaculatus* (Cyprinidae, Teleostei). Submitted for publication.

[3]S.P. Collin, H.B. Collin, and M.A. Ali. 1994. Ultrastructure and organisation of the retina in the cutlips minnow, *Exoglossum maxillingua* (Cyprinidae, Teleostei). Submitted for publication.

was immersion fixed in 4% paraformaldehyde in phosphate buffer (0.1 M) for 40 min. Following fixation and while it was immersed in phosphate buffer, the entire retina of each eye was carefully dissected free of its scleral eyecup and retinal pigment epithelium. The retina was then whole-mounted, ganglion cell layer uppermost, on a 5% gelatinized slide by making a series of peripheral slits in it. The orientation of each retina was noted and confirmed by making a small incision at the dorsal and nasal margins. Each retina was flattened by sandwiching it between the slide on which it was mounted and two pieces of filter paper (Whatman Nos. 1 and 50, both soaked in a 1:1 mixture of formaldehyde and absolute alcohol), a second glass slide, and a brass weight. After drying overnight, the retinal ganglion cell layer was stained for Nissl substance in cold 0.05% cresyl violet (aqueous, pH 4.3) for 4–6 min. Dehydration and clearing then preceded the placing of a cover slip in DePex (Gurr).

Densities of stained cells within the ganglion cell layer were determined for both left and right eyes. Using an Olympus projection microscope, the outline of each retina was traced onto 1 cm^2 grid tracing paper at a magnification of approximately 20 times. The vernier scale on an Olympus compound microscope (BH-2) was then matched to the grid on the tracing paper by noting the positions of obvious landmarks in the whole-mount. A graticule of 100 squares (magnification calibrated for each objective) was placed in the eyepiece and used to define areas for counting at an overall magnification of 1000 times. Cells within each field were routinely counted every 0.05 mm, but in areas of higher density, cells were counted every 0.025 mm on the retina. These numbers were then converted to number of cells per square millimetre. In this way, up to 200 areas per retina were sampled, allowing small fluctuations in cell density to be determined. Isodensity contours were constructed by interpolation between similar values of retinal ganglion cell densities. No allowance was made for shrinkage, which is known to be less than 2% for this technique (Hughes 1975; Mednick and Springer 1988).

All recognizable neural elements lying within the ganglion cell layer were counted. If cellular elements were clearly located between the optic nerve fibre layer and the inner plexiform layer and had some Nissl substance in their cytoplasm, they were counted, independently of size. Therefore, although glial cells, distinguished by their smaller size, cigar shape, and dark staining (Hughes 1985), were not included in cell counts, the densities calculated represent upper limits that may have to be revised downwards when data from retrograde transport studies allow the ganglion cells to be conclusively distinguished from displaced amacrine cells. However, the major contribution of non-ganglion cells has been found to be from peripheral, nonspecialized regions in other teleost retinae in which the topography and the peak densities of teleost retinal ganglion cells have remained relatively unchanged (Collin and Pettigrew 1988c).

Cell soma sizes were determined by means of a camera lucida fitted to an Olympus compound microscope and an IBM graphics tablet. Cellular images, superimposed on a graphics tablet, were outlined with the use of an electronic stylus and each soma area was calculated by computer. Over 250 cells were sampled in each designated area of the retina and collated to produce a histogram of some area versus frequency. Sigma Scan (Jandel Scientific) was used to determine both the area and the total number of cells within the ganglion cell layer by measuring the area bounded by each isodensity contour and multiplying each area by its average cell density.

Results

The creek chub, *Semotilus atromaculatus*, and the cutlips minnow, *Exoglossum maxillingua*, are sympatric cyprinids, but the shape of the pupil and the position of the eyes in the head are different. In *S. atromaculatus* the eyes are placed almost equidistant from the dorsal and ventral surfaces of the head, and subtend a binocular overlap of approximately 20°, and the pupil is circular. The eyes are also placed low in relation to the large mouth (Fig. 2A). In contrast, the eyes of *E. maxillingua* are placed high on the snout, subtend a binocular overlap of approximately 40°, and possess a rostrally tapering pupil (Fig. 1B). Moreover, the mouth is relatively small and modified for capturing bottom-dwelling prey.

Morphology of the retinal ganglion cell layer and overlying vitreal vascularization

The ganglion cell layer (GCL) is thin (22 μm in *S. atromaculatus* and 11 μm in *E. maxillingua*), and consists of either a single (nonspecialized retinal regions) or a double (within the areae centrales) sublamina in both species (Fig. 2). The ganglion cell and nerve fibre layers are subdivided by the endfeet of large Müller cells that extend to the outer limiting membrane. The ganglion cell somata of *S. atromaculatus* form an alternating series of cellular columns or fascicles which are interspersed with bundles of optic axons, while the somata of the GCL in *E. maxillingua* are not fasciculated and are distributed throughout the GCL and the inner plexiform layer. This fasciculation in *S. atromaculatus* is more predominant immediately surrounding the optic nerve head and the pattern is lost with increasing proximity to the retinal periphery.

The retinae of both species possess a well-developed system of vitreal blood vessels. Blood vessels emanate from the ophthalmic artery, which enters the retina with the circular optic nerve. The ophthalmic artery gives way to five large primary arteries which dichotomously divide to form capillaries that supply the entire retina. The ventronasal region receives an increased number of large-calibre vessels, while the temporodorsal region of the retinae of both species receives only small-calibre vessels. The vitreal vessels vary in diameter and overlie between 6 and 7 ganglion cells (primary vessels) and between 1 and 2 ganglion cells (capillaries) in both species (Fig. 2B). Both the capillaries and veins anastomose with the annular collecting vessel that runs along the ora terminalis. Neither of these teleost species possesses a falciform process.

Ganglion cell topography

The distribution of cells within the retinal ganglion cell layer is not uniform throughout the retina of either *S. atromaculatus* or *E. maxillingua*. in *S. atromaculatus* three areas of increased ganglion cell density, defined here as retinal specializations or areae centrales, are found to lie in the dorsonasal (mean peak of 11 496 ± 1167 cells/mm^2, $N = 5$), nasal (mean peak of 12 503 ± 2029 cells/mm^2, $N = 5$), and temporal (mean peak of 14 657 ± 2003 cells/mm^2, $N = 5$) regions of the retina (Figs. 3A, 3B, Table 1). The position of each specialization approximates a triangle with the circular optic nerve head located in the centre and each zone subtending the lower frontal, caudal, and frontal visual fields, respectively. The cell-density gradient between the regions of maximum cell density (areae centrales) and the periphery ranges from 3.0 to 4.3:1 within each retina. The circular optic nerve head is situated centrally and constitutes the hub of incoming alternating fascicles of cell somata (7–10 somata wide) and optic axon bundles. These fascicles, while discretely defined in the central retina, are less defined in the periphery, where the cells in the ganglion cell layer are situated closer to the inner limiting membrane (Figs. 4A, 4B). The total number of cells within the ganglion cell layer is 288 170 ± 4680 ($N = 5$; Table 1). Within the region of peak ganglion cell density (temporal area centralis), the mean soma area is 30.14 ± 10.58 μm^2 ($N = 259$) compared with a mean soma area of 35.72 ± 15.79 μm^2 ($N = 266$) in the

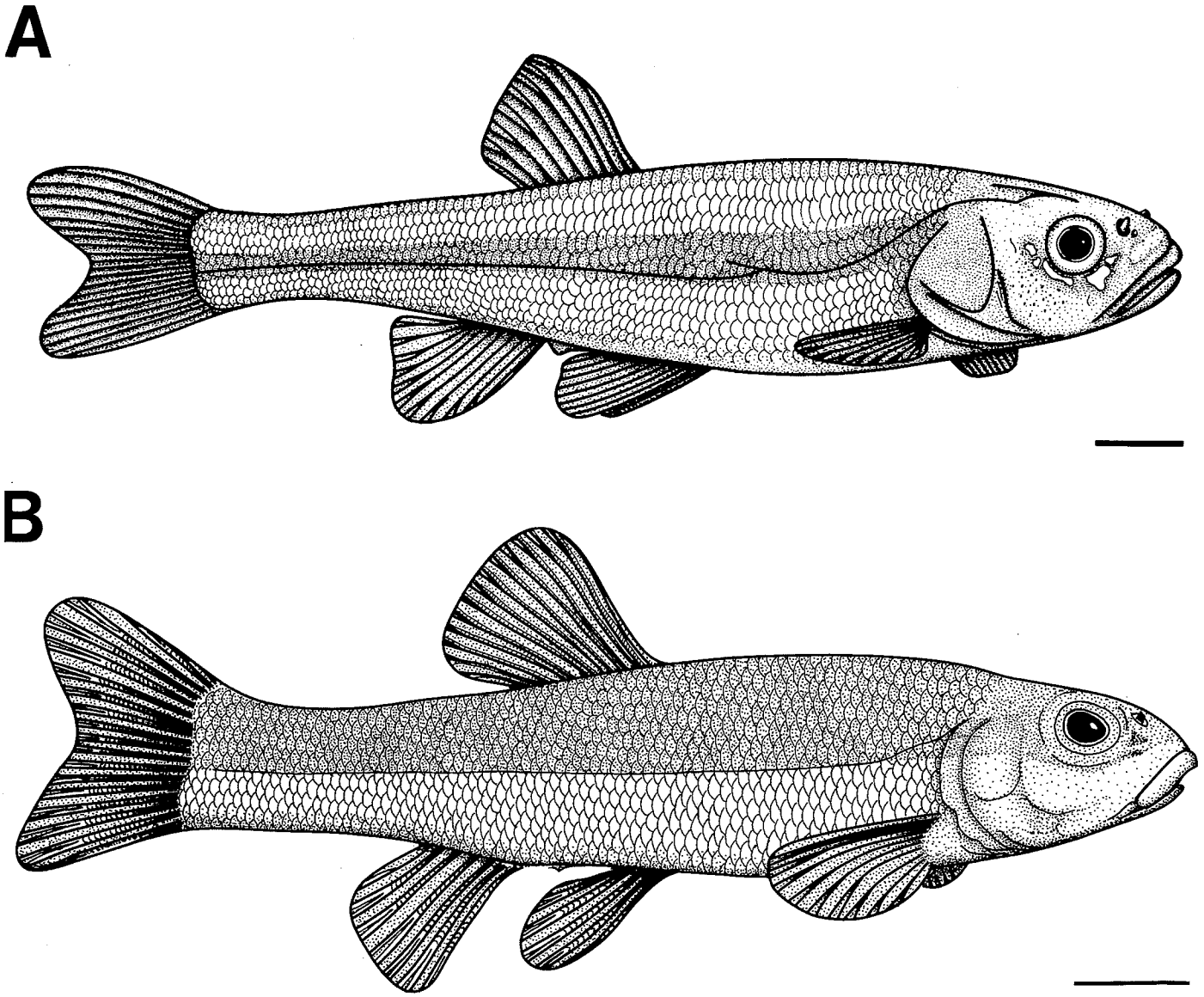

FIG. 1. (A) Lateral view of the creek chub, *Semotilus atromaculatus* (Mitchill) (Cyprinidae). Note the circular pupil. (B) lateral view of the cutlips minnow, *Exoglossum maxillingua* (Lesueur) (Cyprinidae). The pupil is tapered rostrally and the eye is positioned high on the sloping snout. The blunt tapering snout covers a three-lobed mouth used for dislodging bottom-dwelling prey. Scale bars = 1 cm.

nonspecialized peripheral retina (Figs. 5A, 5B). With such a large standard deviation within each retinal region and the high degree of variability in shape, it is likely that this population consists of a number of ganglion cell classes.

In *E. maxillingua*, two areae centrales, one situated in temporal (mean peak of 28 500 ± 400 cells/mm^2; N = 5) and the other in nasal (mean peak of 15 550 ± 2500 cells/mm^2; N = 5) retina, subtend the frontal and caudal visual fields, respectively (Figs. 3C, 3D; Table 1). The cell-density gradient between the region of maximum cell density (temporal area centralis) and the periphery is higher than in *S. atromaculatus* and ranges from 4.3 to 5.6:1 within each retina. It is also interesting to note that the diameter and density of vitreal vascularization is decreased in the temporal region of the retina, i.e., the area occupied by the greatest number of ganglion cells in both species. The total number of cells within the ganglion cell layer in *E. maxillingua* is 261 188 ± 2910 (N = 5; Table 1). The size and shape of the cell soma within the ganglion cell layer are more homogeneous than in *S. atromaculatus*, with most cells situated within the temporo-dorsal area centralis, ranging in soma area between 10 and 20 μm^2 (mean 16.22 ± 3.62 μm^2; N = 250). This compares with a mean soma area of 26.45 ± 8.15 μm^2 (N = 254) in the nonspecialized ventral periphery (Figs. 4C, 4D, 5C, 5D).

Visual spatial resolution

An estimate of the limits of the visual spatial resolution for the two species can be derived from Matthiessen's ratio

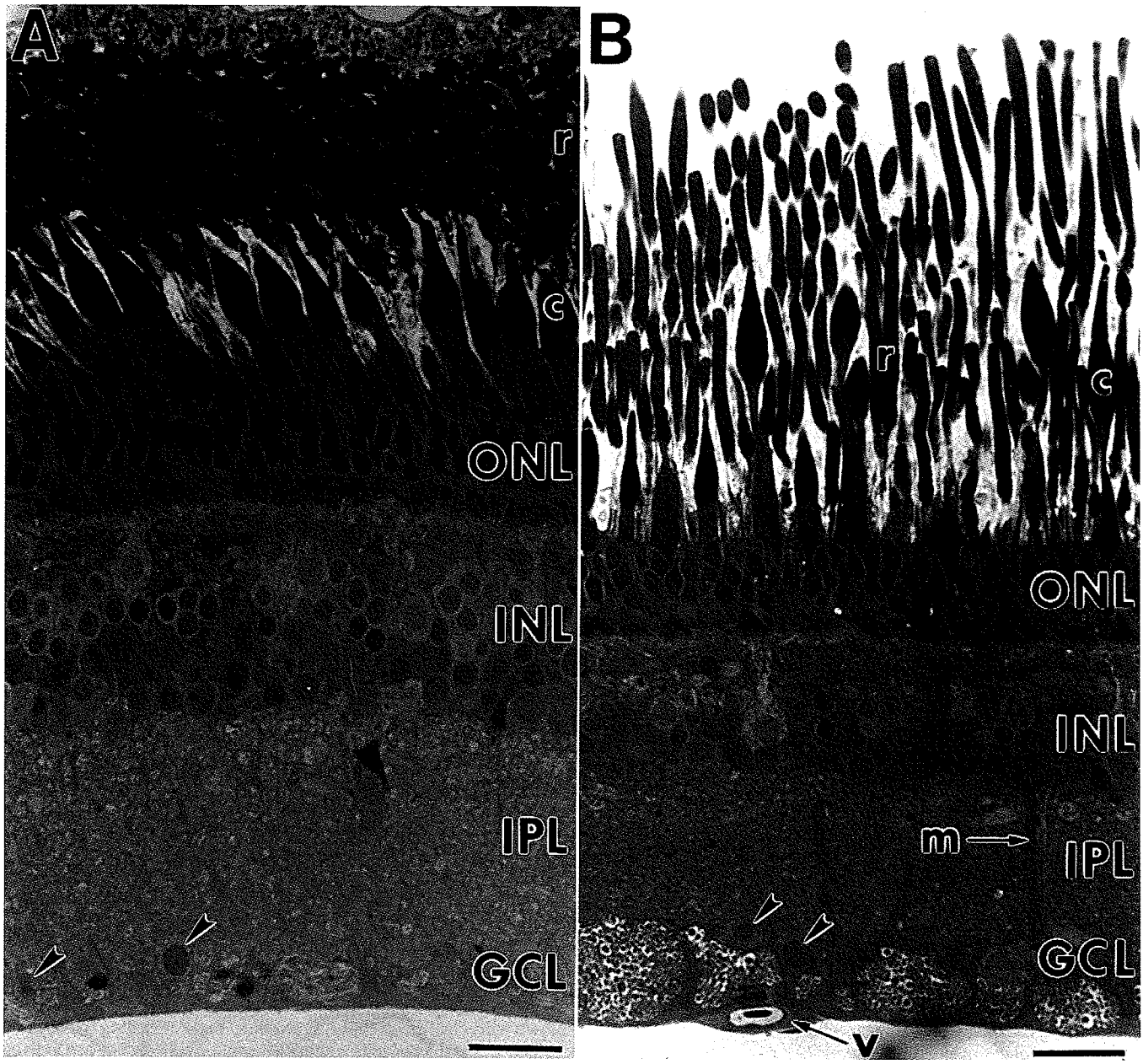

FIG. 2. (A) Transverse section (1 μm) of the light-adapted retina of *S. atromaculatus*, showing the sparse ganglion cells (arrowheads) in the peripheral ganglion cell layer. (B) Transverse section (1 μm) of the dark-adapted retina of *E. maxillingua*, showing the Müller cell endfeet (*m*) that encapsulate the optic axons and divide the ganglion cells (arrowheads). *c*, double and single cones; GCL, ganglion cell layer; INL, inner nuclear layer; IPL, inner plexiform layer; ONL, outer nuclear layer; *r*, rods; *v*, vitreal blood vessel. Scale bars = 20 μm.

(Matthiessen 1880), which states that the distance from the lens centre to the retina (posterior nodal distance, PND) is 2.2–2.8 times the radius of the lens (Collin and Pettigrew 1989). Therefore, the angle (α) subtending 1 mm on the retina can be calculated by obtaining the arc tangent of the reciprocal of the PND (Collin and Pettigrew 1989). The spatial resolution can then be calculated by obtaining the number of cells subtended by 1° of visual arc. The peak number of cells per degree is calculated by dividing the peak ganglion cell densities within the areae centrales by the PND. Since at least two ganglion cells are needed to distinguish the light and dark boundaries forming one cycle of a grating of the highest resolvable frequency, the number of cycles per degree is obtained by dividing the number of cells per degree by two. This method also facilitates the comparison of these two species without the confounding effects of variation in eye size. However, the values obtained represent upper limits that may have to be revised downwards, since the proportion of nonganglion cells (found to be only 8% in the area centralis of *Lienardella fasciata* by Collin and Pettigrew 1988*c*) within the ganglion cell layer is not known for these species.

Semotilus atromaculatus has a peak spatial visual resolution of 2.69–3.99 cycles per degree (using the two extremes of Matthiessen's ratio), while *E. maxillingua* has a resolution of 2.10–3.59 cycles per degree. For both species, the spatial resolving power calculated for the temporal areae centrales was the highest (compared with the other areae), and this value increased with the diameter of the lens (Table 1).

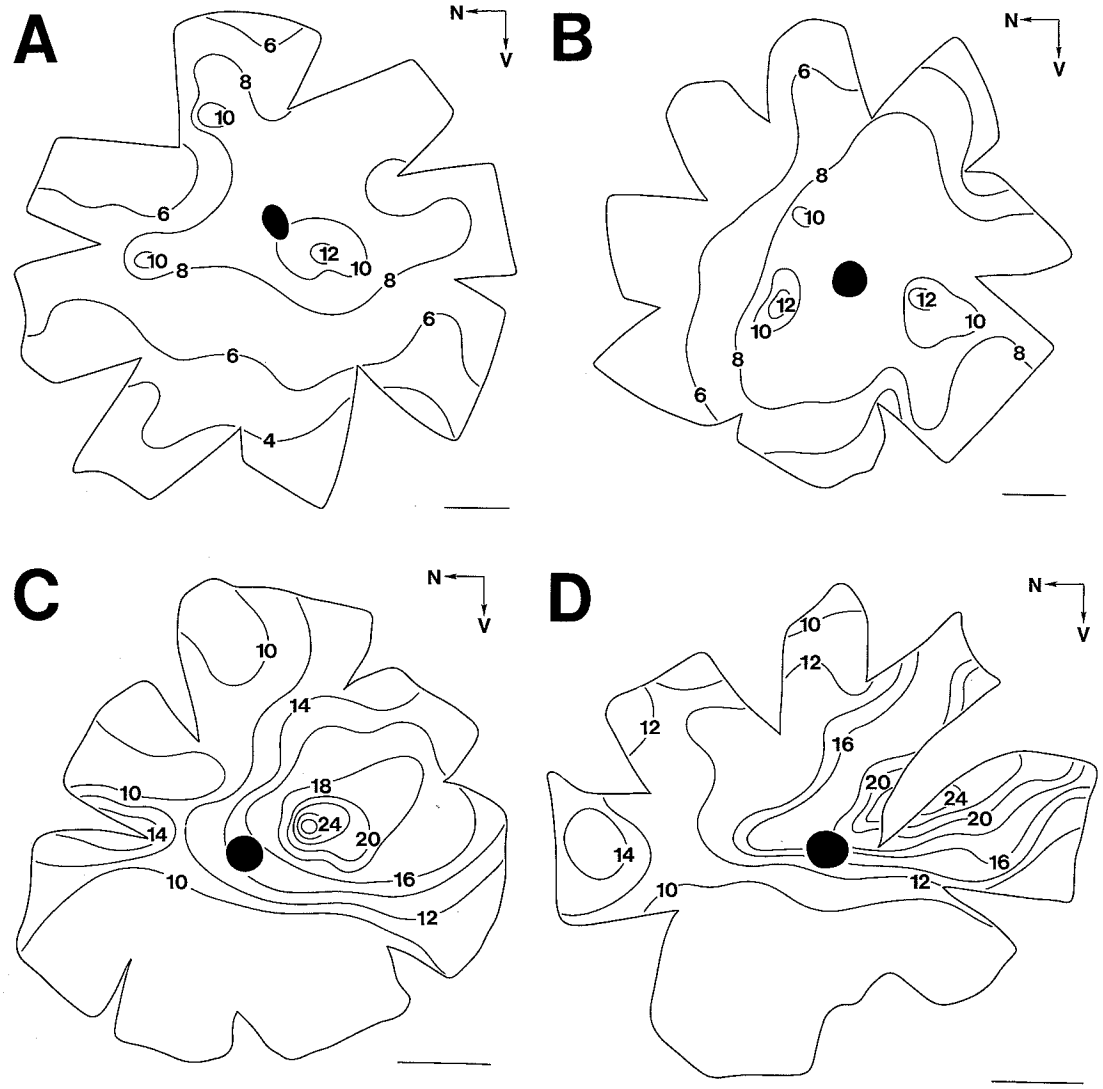

FIG. 3. (A, B) Retinal topography of cells within the ganglion cell layer of two individual creek chubs, *S. atromaculatus*, revealing the three areas of greater cell density surrounding the optic nerve head (black area). (C, D) Retinal topography of cells within the ganglion cell layer of two individual cutlips minnows, *E. maxillingua*, revealing a pronounced increase in cell density in temporal and nasal retina. All isodensity contour maps are of the left eye. Densities are $\times 10^3$ cells/mm^2. N, nasal; V, ventral. Scale bars = 1 mm.

TABLE 1. Sample data calculated for two individuals of each species summarizing the retinal acute zones

	Size (mm)	Position of area centralis	Peak cell density ($\times 10^3$ cells/mm^2)	Acuity[a] (cycles per degree)	Lens diam. (mm)	Total cell number ($\times 10^5$)
Semotilus atromaculatus	110	Dorsonasal	13.08	2.76–3.45	2.45	2.94
		Nasal	14.97	2.86–3.58		
		Temporal	17.46	3.18–3.99		
	108	Dorsonasal	11.11	2.83–3.56	2.39	2.83
		Nasal	10.00	2.69–3.37		
		Temporal	13.61	3.08–3.45		
Exoglossum maxillingua	95	Nasal	15.30	2.11–2.61	1.83	2.57
		Temporal	28.90	2.90–3.59		
	95	Nasal	15.80	2.10–2.60	1.79	2.62
		Temporal	28.10	2.80–3.46		

[a] Range according to the range of Matthiessen's ratio (Matthiessen 1880).

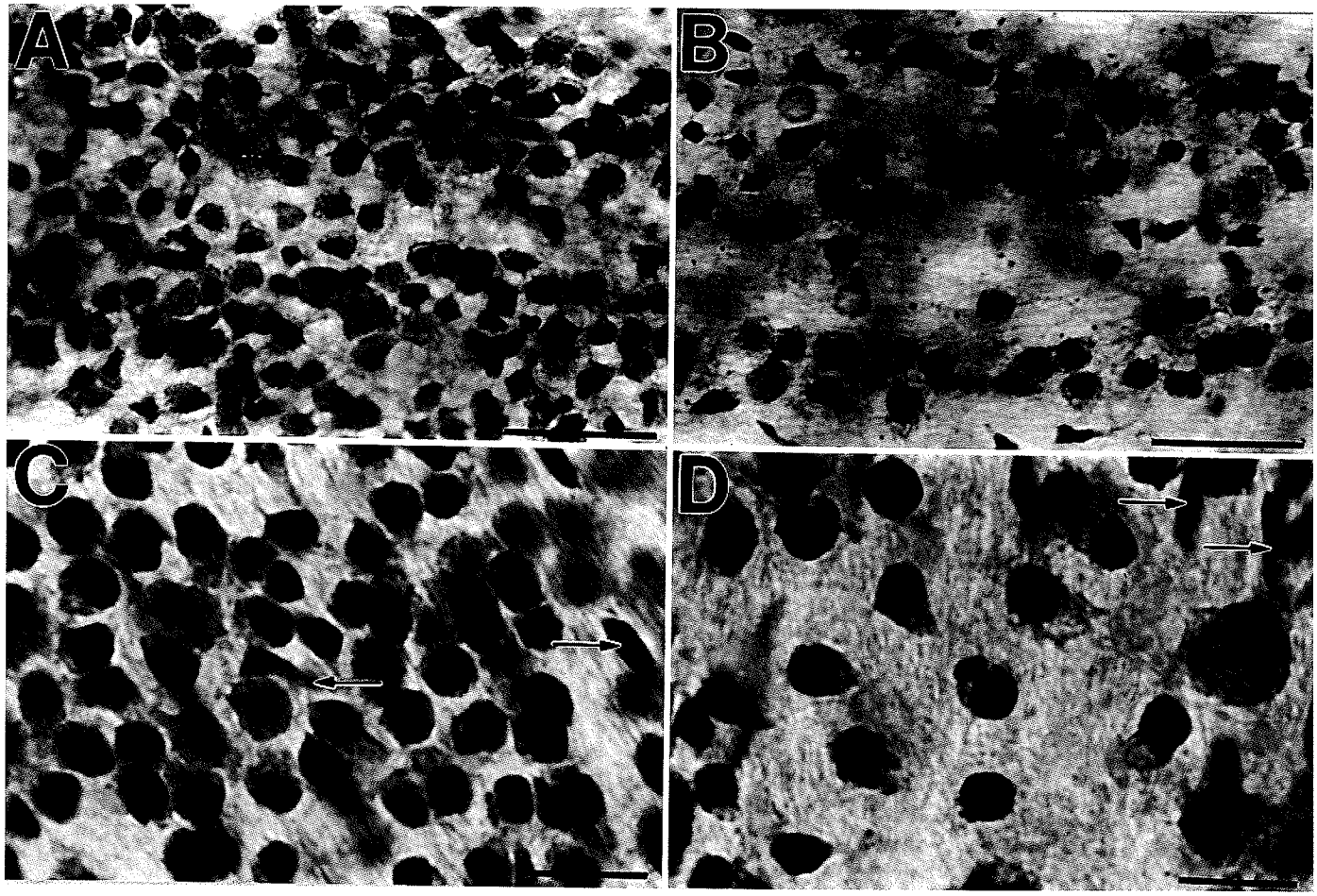

FIG. 4. Light micrographs of all the neuronal elements stained for Nissl substance in the ganglion cell layer of *S. atromaculatus* (A, B) and *E. maxillingua* (C, D) in various regions of the retina. (A) The temporal area centralis. (B) The nasal periphery. (C) The temporal area centralis. (D) The ventral periphery. The arrows depict glial cells, which were omitted in all cell counts. Scale bars: 30 μm in A and B; 10 μm in C and D.

Discussion

The retinae of both the creek chub, *Semotilus atromaculatus*, and the cutlips minnow, *Exoglossum maxillingua*, possess multiple areas of increased cell density within the ganglion cell layer. In spite of the close phylogenetic relationship between the two cyprinid species, each retina possesses a unique distribution. Since the maximum density of cells sampled increases to at least four times that of peripheral densities and the proportion of nonganglion cells in these regions is thought to be approximately 8% (Collin and Pettigrew 1988*c*), these specialized regions may provide these species with increased acuity in different parts of their visual field. The photoreceptor sampling, oculomotor range, and accommodative lens movements must now be investigated in detail to finally confirm whether these areae are actively used in the fishes' visual behaviour.

Other studies on retinal topography in cyprinid species reveal retinal specializations with a temporal area centralis of 5.661×10^3 ganglion cells/mm^2 in the goldfish *C. auratus* (Mednick and Springer 1988). Two areae centrales are found in the adult roach *Rutilus rutilus* (6.3×10^3 cones/mm^2 temporal and 5.5×10^3 cones/mm^2 nasal), the carp *Cyprinus carpio* (8.8×10^3 cones/mm^2 temporal and 8.3×10^3 cones/mm^2 nasal), the bream *Abramis brama* (6.0×10^3 cones/mm^2 temporal and 4.8×10^3 cones/mm^2 dorsonasal), the asp, *Aspius aspius* (9.9×10^3 cones/mm^2 temporoventral and 5.1×10^3 cones/mm^2 dorsonasal), and the sabre carp, *Pelecus cultratus* (10.8×10^3 cones/mm^2 temporoventral and 8.9×10^3 cones/mm^2 dorsonasal (Zaunreiter et al. 1991). Therefore, a diverse range of retinal specializations has evolved in cyprinids, emphasising the important role vision plays in these species' survival.

A distinct advantage of multiple retinal areae is that an organism could perceive its visual world with higher resolution without the saccadic eye movements necessitated by a single area centralis. This means that the dorsonasal and nasal areae of *S. atromaculatus* and the nasal area of *E. maxillingua*, although not providing maximum-acuity vision, may still function in providing each species with a means to perceive potential predators and (or) prey. The arrangement of isodensity contours of both species also reveals pronounced variation. *Semotilus atromaculatus* possesses a concentric arrangement of isodensity contours surrounding three foci. In contrast, the topography of the isodensity contours of *E. maxillingua* reveals a distinct elongation along the horizontal meridian of the retina. Theoretically, this variation in topography may be associated with each species' chosen ecological niche: midwater (*S. atromaculatus*) versus benthic (*E. maxillingua*). In this scenario, the elongation of isodensity contours in *E. maxillingua* may reflect its perceived environment, its horizon being the interface between the water and the bottom

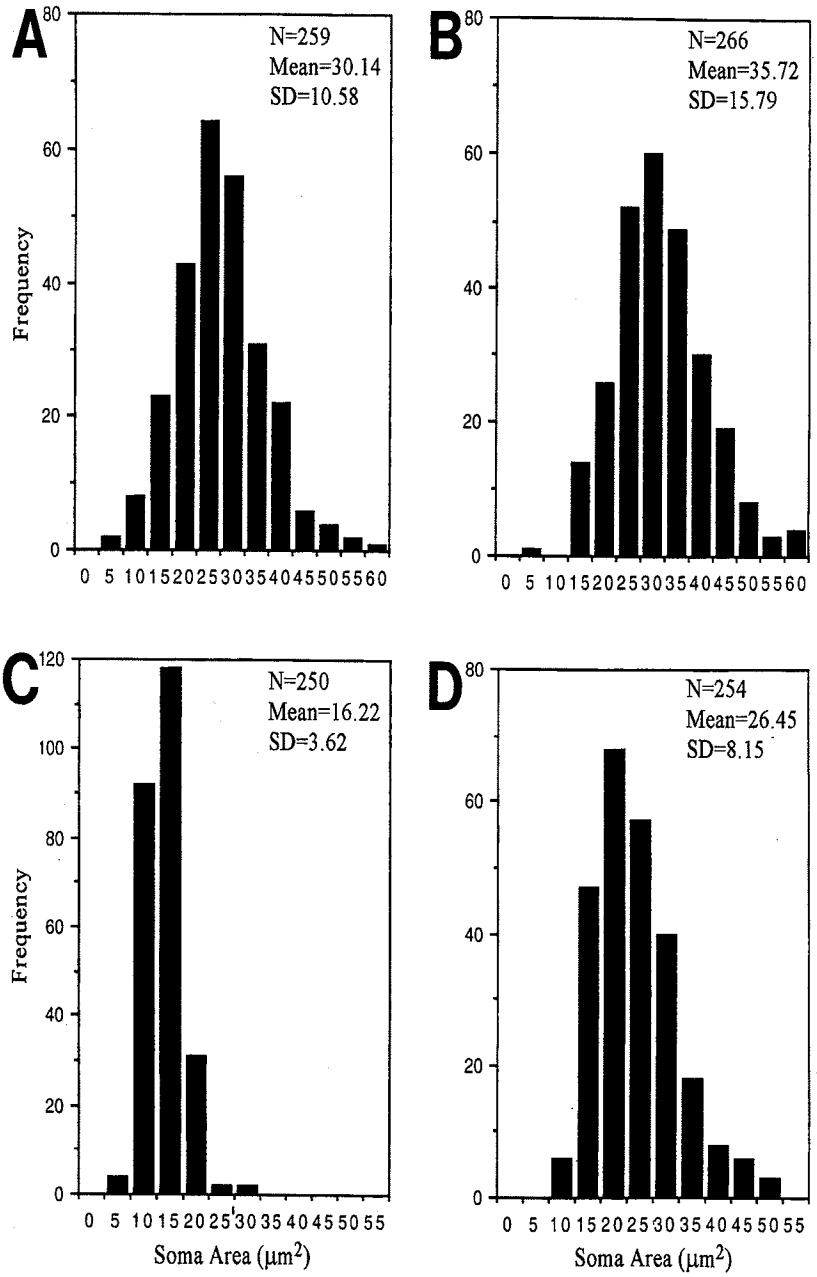

FIG. 5. Frequency versus soma size for all neuronal elements (excluding glial cells) that lie within the ganglion cell layer of *S. atromaculatus* (A, B) and *E. maxillingua* (C, D) in specialized and nonspecialized regions of the retina. (A) The temporal area centralis. (B) The nasal periphery. (C) The temporal area centralis. (D) The ventral periphery.

of the lake, where it spends over 80% of its time and from which it feeds. For *S. atromaculatus*, concentric contours reflect the three-dimensional visual environment of this species, which favours the mid to upper regions of the water column. A similar relationship has been described for teleosts in a reef ecosystem (Collin and Pettigrew 1988*a*, 1988*b*) and for a range of terrestrial vertebrates (Hughes 1977), where the symmetry of each animal's perceived world is closely reflected by the arrangement of retinal ganglion cells.

The observation of three areae centrales in the retina of *S. atromaculatus* is only the second such finding for vertebrates and poses interesting questions regarding the development of these areae. Three areae centrales have been found in the marine staghorn damsel fish, *Amblyglyphidodon curacao*, which possesses regions of higher cell density within the ganglion cell layer in temporal (2.5×10^4 cells/mm^2), ventrotemporal (3.0×10^4 cells/mm^2), and dorsonasal (2.3×10^4 cells/mm^2) retina (Collin and Pettigrew 1988*a*). Like *S. atromaculatus*, this species also inhabits the upper layers of the water column and feeds on minute moving prey. The spatial resolving power of the temporal area centralis in the two species also compares favourably (6–8 cycles per degree in *A. curacao* versus 3–4 cycles per degree in *S. atromaculatus*), although one would expect higher acuity in *A. curacao*, given a 40% increase in cell density in a comparably sized eye.

A comparison of estimates of spatial resolution for *S. atromaculatus* (2.76–3.99) and *E. maxillingua* (2.10–3.59) with measurements made in the regions of highest cone density (Van der Meer and Anker 1984) in other members of

the cyprinid family shows remarkable similarity. *Rutilus rutilus* (2.50 cycles per degree), *C. carpio* (3.69 cycles per degree), *A. brama* (3.96 cycles per degree), and *A. aspius* (3.52 cycles per degree) all have values within the range described for the two species in this study. The exception is *P. cultratus*, which possesses a resolving power of 5.31 cycles per degree (Zaunreiter et al. 1991).

Although, the retinae of both species possess multiple areas of acute vision as adults (this study), the arrangement may be quite different in juvenile stages. Different stages of *S. atromaculatus* adopt a layered distribution pattern within the water column. In large pools, bigger creek chub occupy deeper areas of water and the younger, smaller fish occupy the upper levels (Copes 1978). Smaller juvenile creek chub (20–60 mm in length) are essentially diurnal, feeding on small prey (dipterans and ephemeropterans), and are mainly found in shallow littoral water (0.8 m depth). However, adults (61–81+ mm in length) are principally nocturnal, shifting their attention to the larger, robust larvae of tipulid and stratiomyid dipterans and caddisflies, and are found in deeper waters (1.2–2.9 m depth; Magnan and FitzGerald 1984*a*). Invertebrates such as molluscs and other fish also make up the bulk of the diet of the largest individuals (Barber and Minckley 1971).

Similarly, a shift in feeding preference is observed for *E. maxillingua*, smaller fish prefering chironomids and the larger specimens prefering the larger trichopteran larvae, especially hydropsychids (Pappantoniou et al. 1984*a*), oligochaetes, asticids, and taeniopterygids (Pappantoniou et al. 1984*b*). During development the cutlips minnow also undergoes an accelerated increase in body size (up to 15 mm in total length), which alters proportional head measurements (Fuiman and Loos 1978) and changes the relative position of the eyes of the mouth (Fig. 1B). It is not known whether the retinal topography changes throughout development in these two species, but pronounced changes in feeding strategy and habitat throughout life suggest that it may.

The development of such an arrangement of acute zones in these species is not known but must involve a combination of passive stretching as the eye grows in size and new cells are actively added at the periphery (Johns and Easter 1977). However, how are the central positions of the three acute zones in *S. atromaculatus* and the two peripheral acute zones in *E. maxillingua* maintained? Easter (1992) suggests that there are two types of retinal growth in marine teleosts, symmetric and asymmetric, which may explain the retinal growth in these two species. During symmetric retinal growth, annuli of ganglion cells are added concentrically to ganglion cells where the distance between any two annuli is the same in all regions of the retina. During asymmetric growth, however, although the annuli of cells are still added peripherally, the nasal annuli are spaced farther apart than the temporal annuli (Easter 1992). In this way, a temporal area centralis or fovea is maintained and subserves a frontal visual field without the need for frontal migration of the two eyes during development (eye migration has not been examined in either *S. atromaculaus* or *E. maxillingua*).

Presumably, asymmetric retinal growth may account for the appearance of the temporal and nasal acute zone in *E. maxillingua*, since some variation in the degree of asymmetric growth was observed in species possessing two acute zones (e.g., *Parapercis cylindrica*; Collin and Pettigrew 1988*a*; Easter 1992). The development of the multiple acute zones of *S. atromaculatus* is more difficult to explain. Easter (1992) considers that the acute zones of the damselfish *A. curacao* (centroperipheral gradient of 3.2:1; Collin and Pettigrew 1988*a*), the goldfish *C. auratus* (centroperipheral gradient of 2.5:1, Mednick and Springer 1988), and the rippled blenny, *Istiblennius edentulus* (centroperipheral gradient of 3.2:1; Collin 1989), may not be significant, statistically or functionally. This implies that the retinae of these species develop by a process of symmetric growth.

The examination of intraspecific variation in this study suggests that these areae *are* statistically significant and reproducible (in Nissl stained cell counts). Therefore, these retinal areae may each provide increased sampling of an image in different regions of the visual field, given that the photoreceptors follow a similar topographic pattern. Behavioural and electrophysiological studies must now be undertaken to determine whether these zones are functional, sampling different regions of the visual field. It is possible that the cells within these zones are processing other elements of the visual field i.e., spatiotemporal information. If the retinae of *S. atromaculatus* and *A. curacao* develop by a process of symmetric growth, which may be possible given the symmetric positioning of the three areae centrales around the optic nerve head, there must still be some differential retinal expansion surrounding the three foci. Developmental studies of retinal growth utilizing retrograde labelling from the optic nerve will undoubtedly shed new light on this problem.

Acknowledgements

The authors thank Luc Beaudet, Peter Heinermann, and Damijana Ota for their assistance in the collection and fixation of this material. They also extend their appreciation to Robert Beausejour and the staff of the Station de Biologie, Université de Montréal. S.P. Collin was supported partly by an operating grant from the Natural Sciences and Engineering Research Council of Canada (NSERC) to M.A. Ali and later by both a C.J. Martin Fellowship from the National Health and Medical Research Council of Australia and a Fulbright Postdoctoral Fellowship from the Australian–American Educational Foundation. This research was funded by grants from NSERC and Formation de chercheurs et l'áide à la recherche to M.A. Ali.

Ahlbert, I.-B. 1976. Organization of the cone cells in the retinae of salmon (*Salmo salar*) and trout (*Salmo trutta trutta*) in relation to their feeding habits. Acta Zool. (Stockholm), **57**: 13–35.

Barber, W.E., and Minckley, W.L. 1971. Summer foods of the cyprinid fish *Semotilus atromaculatus*. Trans. Am. Fish. Soc. 1971: 283–289.

Cerri, R.D. 1983. The effect of light intensity on predator and prey behaviour in cyprinid fish: factors that influence prey risk. Anim. Behav. **31**: 736–742.

Collin, S.P. 1989. Topographic organization of the ganglion cell layer and intraocular vascularization in the retinae of two reef teleosts. Vision Res. **29**: 765–775.

Collin, S.P., and Collin, H.B. 1988. Topographic analysisof the retinal ganglion cell layer and optic nerve in the sandlance *Limnichthyes fasciatus* (Creeiidae, Perciformes). J. Comp. Neurol. **278**: 226–241.

Collin, S.P., and Pettigrew, J.D. 1988*a*. Retinal topography in reef teleosts. I. Some species with well developed areae but poorly-developed streaks. Brain Behav. Evol. **31**: 269–282.

Collin, S.P., and Pettigrew, J.D. 1988*b*. Retinal topography in reef teleosts. II. Some species with prominent horizontal streaks and high density areae. Brain Behav. Evol. **31**: 283–295.

Collin, S.P., and Pettigrew, J.D. 1988*c*. Retinal ganglion cell topography in teleosts: a comparison between Nissl-stained material and retrograde labelling from the optic nerve. J. Comp. Neurol. **276**: 412–422.

Collin, S.P., and Pettigrew, J.D. 1989. Quantitative comparison of the limits on visual spatial resolution set by the ganglion cell layer in twelve species of reef teleosts. Brain Behav. Evol. **34**: 184–192.

Copes, F.C. 1978. Ecology of the creek chub. *In* Reports on the flora and fauna of Wisconsin No. 12. *Edited by* G.C. Becker and C.A. Long. The Museum of Natural History, University of Wisconsin, Stevens Point, pp. 1–21.

Dinsmore, J.J. 1962. Life history of the creek chub, with emphasis on growth. Iowa Acad. Sci. **69**: 296–301.

Dobis, J.O., Meehean, L., Snieszko, S.F., and Washburn, G.N. 1956. Raising bait fishes. U.S. Fish Wildl. Serv. Circ. No. 35.

Dunlop, S.A., and Beazley, L.D. 1981. Changing retinal ganglion cell distribution in the frog *Heleiporus eyrei*. J. Comp. Neurol. **202**: 221–236.

Easter, S.S., Jr. 1992. Retinal growth in foveated teleosts: nasotemporal asymmetry keeps the fovea in temporal retina. J. Neurosci. **12**: 2381–2392.

Evans, H.E. 1952. The correlation of brain pattern and feeding habits in four species of cyprinid fishes. J. Comp. Neurol. **97**: 133–142.

Fernald, R.D., and Johns, P.R. 1980. Retinal specialization and growth in the cichlid fish, *Haplochromis burtoni*. Am. Zool. **20**: 943.

Fuiman, L.A., and Loos, J.J. 1978. Morphological changes during the larval development of the cutlips minnow, *Exoglossum maxillingua*. Trans. Am. Fish. Soc. **107**: 605–612.

Hankinson, T.L. 1922. Nest of cutlips minnow, *Exoglossum maxillingua* (LeSueur). Copeia, **102**: 1–3.

Hebel, R., and Hollander, H. 1983. Size and distribution of ganglion cells in the human retina. Anat. Embryol. **168**: 125–136.

Heinermann, P.H., and Ali, M.A. 1985. Correlation between the photic environment and prophyropsin in the cutlips minnow, *Exoglossum maxillingua*. Naturwissenschaften, **72**: 488–489.

Heinermann, P.H., and Ali, M.A. 1989. The photic environment and scotopic visual pigments of the creek chub, *Semotilus atromaculatus* and white sucker, *Catostomus commersoni*. J. Comp. Physiol. A, **164**: 707–716.

Hughes, A. 1975. A quantitative analysis of the cat retinal ganglion cell topography. J. Comp. Neurol. **163**: 107–128.

Hughes, A. 1977. The topography of vision in mammals of contrasting life styles: comparative optics and retinal organisation. *In* The visual system of vertebrates. *Edited by* F. Crescitelli. Springer-Verlag, New York. pp. 613–756.

Hughes, A. 1985. New perspectives in retinal organization, *In* Progress in retinal research. *Edited by* N.N. Osborne and G. Chader. Pergamon Press, New York. pp. 243–313.

Ito, H., and Murakami, T. 1984. Retinal ganglion cells in two teleost species, *Sebastiscus marmoratus* and *Navodon modestus*. J. Comp. Neurol. **229**: 80–96.

Johns, P.R., and Easter, S.S., Jr. 1977. Growth of the adult goldfish eye. II. Increase in retinal cell number. J. Comp. Neurol. **176**: 331–342.

Johnson, J.H. 1981. The summer diet of the cutlips minnow, *Exoglossum maxillingua*, in a central New York stream. Copeia, 1981: 484–487.

Johnson, J.H. 1982. Obsservations on the eye picking behaviour of the cutlips minnow, *Exoglossum maxillingua*. Copeia, 1982: 711–712.

Kahmann, H. 1934. Über das Vorkommen einer Fovea centralis im Knochenfischauge. Zool. Anz. **106**: 49–55.

Kahmann, H. 1935. Über das foveale Sehen der Wirbeltiere. II. Gesichtsfeld und Fovea centralis. Sitzungsber. Ges. Naturforsch. Freunde Berlin. pp. 361–376.

Kawamura, G., and Ohashi, S. 1988. The habit of cutlassfish as inferred from the retina. Nippon Suisan Gakkaishi, **54**: 889.

Koch, J.-H., and Reuter, T. 1978. Retinal ganglion cells in the crucian carp (*Carassius carassius*). I. Size and number of somata in eyes of different sizes. J. Comp. Neurol. **179**: 535–548.

Magnan, P., and FitzGerald, G.J. 1982. Resource partitioning between brook trout (*Salvelinus fontinalis* Mitchill) and creek chub (*Semotilus atromaculatus* Mitchill) in selected oligotrophic lakes of southern Quebec. Can. J. Zool. **60**: 1612–1617.

Magnan, P., and FitzGerald, G.J. 1984*a*. Ontogenetic changes in diel activity, food habits and spatial distribution of juvenile and adult creek chub, *Semotilus atromaculatus*. Environ. Biol. Fishes, **11**: 301–307.

Magnan, P., and FitzGerald, G.J. 1984*b*. Mechanisms responsible for the niche shift of brook charr, *Salvelinus fontinalis* Mitchill, when living sympatrically with creek chub, *Semotilus atromaculatus* Mitchill. Can. J. Zool. **62**: 1548–1555.

Matthiessen, L. 1880. Untersuchungen über dem Aplanatismus und die Periscopie der Kristallinsen in den Augen der Fische. Pfluegers Arch. **21**: 287–307.

Mednick, A.S., and Springer, A.D. 1988. Asymmetric distribution of retinal ganglion cells in goldfish. J. Comp. Neurol. **268**: 49–59.

Mednick, A.S., Berk, M.F., and Springer, A.D. 1988. Asymmetric distribution of cells in the inner nuclear and cone mosaic layers of the goldfish retina. Neurosci. Lett. **94**: 241–246.

Munk, O. 1970. On the occurrence and significance of horizontal band-shaped retinal areae in teleosts. Vidensk. Medd. Dan. Naturhist. Foren. **133**: 85–120.

Murray, M., Sharma, S.C., and Edwards, M.A. 1982. Target regulation of synaptic number in the compressed retinotectal projection of goldfish. J. Comp. Neurol. **209**: 374–385.

O'Connell, C.P. 1963. The structure of the eye of *Sardinops caerulea*, *Engraulis mordax* and four other pelagic marine teleosts. J. Morphol. **113**: 287–330.

Pappantoniou, A., Schmidt, R.E., and Dale, G. 1984*a*. Ecology and life history of the cutlips minnow, *Exoglossum maxillingua*, from a southeastern New York stream. Northeast. Environ. Sci. **3**: 75–79.

Pappantoniou, A., Dale, G., and Schmidt, R.E. 1984*b*. Aspects of the life history of the cutlips minnow, *Exoglossum maxillingua*, from two eastern Pennsylvania streams. J. Freshwater Ecol. **2**: 449–458.

Reighard, J. 1910. The breeding habits of the horned dace and methods of studying the habits of fishes. Bull. U.S. Bur. Fish. **28**: 1111–1136.

Schwassmann, H.O. 1968. Visual projections upon the optic tectum in foveate marine teleosts. Vision Res. **8**: 1337–1348.

Scott, W.B., and Crossman, E.J. 1973. Freshwater fishes of Canada. Fish. Res. Board Can. Bull. No. 184.

Slonaker, J.R. 1897. A comparative study on the area of acute vision in vertebrates. J. Morphol. **13**: 445–503.

Van der Meer, H.J., and Anker, G.C. 1984. Retinal resolving power and sensitivity of the photopic system in seven haplochromine species (Teleostei, Cichlidae). Neth. J. Zool. **34**: 197–209.

Van Duzer, E.M. 1939. Observations on the breeding habits of the cutlips minnow, *Exoglossum maxillingua*. Copeia, 1939: 65–75.

Vaney, D.I. 1980. A quantitative comparison between the ganglion cell populations and axonal outflows of the visual streak and periphery of the rabbit retina. J. Comp. Neurol. **189**: 215–233.

Wong, R.O.L., Wye-Dvorak, J., and Henry, G.H. 1986. Morphology and distribution of neurons in the retinal ganglion cell layer of the adult tammar wallaby *Macropus eugenii*. J. Comp. Neurol. **253**: 1–12.

Yamanouchi, T. 1956. The visual acuity of the coral fish, *Microcanthus strigatus* (Cuvier Valenciennes). Publ. Seto Mar. Biol. Lab. **5**: 133–156.

Yoon, M., Leblanc, R.M., Ali, M.A., and Heinermann, P.H. 1988. Low-temperature photoacoustic spectroscopy of porphyropsin in the intact retina of the creek chub, *Semotilus atromaculatus*. Photochem. Photobiol. **48**: 549–552.

Zaunreiter, M., Junger, H., and Kotrschal, K. 1991. Retinal morphology of cyprinid fishes: a quantitative histological study of ontogenetic changes and interspecific variation. Vision Res. **31**: 383–394.